HHS Public Access

Author manuscript

Adv Exp Med Biol. Author manuscript; available in PMC 2015 June 04.

Published in final edited form as:

Adv Exp Med Biol. 2014 ; 801: 637–645. doi:10.1007/978-1-4614-3209-8_80.

Very Long Chain Polyunsaturated Fatty Acids and Rod Cell Structure and Function

L.D. Marchette,
Department of Cell Biology, University of Oklahoma Health Sciences Center, Oklahoma City, OK 73104, USA; Dean McGee Eye Institute, University of Oklahoma Health Sciences Center, 608 Stanton L. Young Blvd., Oklahoma City, OK 73104, USA

D.M Sherry,
Department of Cell Biology, University of Oklahoma Health Sciences Center, Oklahoma City, OK 73104, USA; Oklahoma Center for Neuroscience, University of Oklahoma Health Sciences Center, Oklahoma City, OK 73104, USA; Department of Pharmaceutical Sciences, University of Oklahoma Health Sciences Center, Oklahoma City, OK 73104, USA

R. S Brush,
Department of Ophthalmology, University of Oklahoma Health Sciences Center, Oklahoma City, OK 73104, USA; Dean McGee Eye Institute, University of Oklahoma Health Sciences Center, 608 Stanton L. Young Blvd., Oklahoma City, OK 73104, USA

M. Chan,
Department of Ophthalmology, University of Oklahoma Health Sciences Center, Oklahoma City, OK 73104, USA; Dean McGee Eye Institute, University of Oklahoma Health Sciences Center, 608 Stanton L. Young Blvd., Oklahoma City, OK 73104, USA

Y. Wen,
Amherst College, Amherst, MA, USA

J. Wang,
University of Florida, Gainesville, FL, USA

John D. Ash,
University of Florida, Gainesville, FL, USA

Robert E. Anderson, and
Department of Ophthalmology, University of Oklahoma Health Sciences Center, Oklahoma City, OK 73104, USA; Department of Cell Biology, University of Oklahoma Health Sciences Center, Oklahoma City, OK 73104, USA; Dean McGee Eye Institute, University of Oklahoma Health Sciences Center, 608 Stanton L. Young Blvd., Oklahoma City, OK 73104, USA

N. A. Mandal
Department of Ophthalmology, University of Oklahoma Health Sciences Center, Oklahoma City, OK 73104, USA; Dean McGee Eye Institute, University of Oklahoma Health Sciences Center, 608 Stanton L. Young Blvd., Oklahoma City, OK 73104, USA

Correspondence to: N. A. Mandal, mmandal@ouhsc.edu.

L.D. Marchette: leamarchette@ouhsc.edu; D.M Sherry: david-sherry@ouhsc.edu; R. S Brush: Richard-Brush@ouhsc.edu; M. Chan: michael-chan@ouhsc.edu; Y. Wen: YWen15@Amherst.edu; J. Wang: garywang@ufl.edu; N. A. Mandal: mmandal@ouhsc.edu

Abstract

The gene encoding Elongation of Very Long Chain Fatty Acids-4 (ELOVL4) is mutated in patients with autosomal dominant Stargardt's Macular Dystrophy Type 3 (STDG3). ELOVL4 catalyzes the initial condensation step in the elongation of polyunsaturated fatty acids (PUFA) containing more than 26 carbons (26C) to very long chain PUFA (VLC-PUFA; C28 and greater). To investigate the role of VLC-PUFA in rod photoreceptors, we generated mice with rod-specific deletion of *Elovl4* (RcKO). The mosaic deletion of rod-expressed ELOVL4 protein resulted in a 36 % lower amount of VLC-PUFA in the retinal phosphatidylcholine (PC) fraction compared to retinas from wild-type mice. However, this reduction was not sufficient to cause rod dysfunction at 7 months or photoreceptor degeneration at 9 or 15 months.

Keywords

ELOVL4; VLC-PUFA; Photoreceptor; ERG; Rod

80.1 Introduction

The fatty acid condensing enzyme Elongation of Very Long Chain Fatty Acids-4 (ELOVL4) is mutated in patients with the autosomal dominant Stargardt's Macular Dystrophy Type 3 (STDG3) [1]. ELOVL4 is expressed in skin, brain, testis, and retina and is responsible for the initial rate-limiting step to elongate fatty acid species with more than 26 acyl carbons (C26) [2]. ELOVL4 expression in skin produces very long chain (VLC)-saturated fatty acids, whereas ELOVL4 in brain, testis, and retina produces VLC-PUFA (VLC-PUFA; C28-C38). To investigate the role of VLC-PUFA in rod photoreceptors, we conditionally deleted *Elovl4* in mouse rod photoreceptor cells.

80.2 Materials and Methods

80.2.1 Animal Use

Mice with LoxP sites flanking exon 5 of the *Elovl4* ($ELO^{flox/flox}$) gene were mated with transgenic mice expressing Cre recombinase (Cre) driven by the rhodopsin promoter [3] ($ELO^{flox/flox}$ mice were a gift from Dr. Kang Zhang, USC, San Diego, CA). Progeny were backcrossed to $ELO^{flox/flox}$ to ultimately generate a rod-specific conditional knock out ($Cre^{+}/ELO^{flox/flox}$; RcKO) and littermate control wild-type ($Cre^{-}/ELO^{flox/flox}$; WT) mice. Mice were housed in a 12 h light ON (20 lx)/OFF cycle. All procedures were performed according to the Association for Research in Vision and Ophthalmology Statement for the Use of Animals in Ophthalmic and Vision Research and protocols were approved by the Institutional Animal Care and Use Committees of the University of Oklahoma Health Sciences Center and the Dean McGee Eye Institute.

80.2.2 Immunolabeling of Retinal Wholemounts

Retinal wholemounts were immunolabeled as described previously [4] using the following primary antibodies: anti-ELOVL4 (1:200) [2], anti-Cre recombinase (Cre; 1:500; Abcam), and anti-cone arrestin (1:500; Gift of Dr. Cheryl Craft, USC, Los Angeles, CA). Labeling was visualized using appropriate fluorescent secondary antibodies (1:200; Invitrogen-Molecular Probes), and imaged using an Olympus BX61-WI microscope (Olympus America) with an ORCA-ER camera (Hamamatsu America) controlled by Slidebook software (Intelligent Imaging Innovations). Brightness and contrast were adjusted to highlight specific labeling using Photoshop (Adobe Systems). Images were analyzed by ImageJ software.

80.2.3 Tandem Mass Spectrometry Analysis of Retina Lipids

The methods have been described previously [5]. Briefly, one mouse retina per sample was homogenized in 40 % aqueous methanol and diluted 1:20 with 2-propanol/methanol/chloroform (4:2:1 v/v/v) containing 20 mM ammonium formate and 1.00 μM phosphatidylcholine (PC, 14:0/14:0) as an internal standard. Samples were introduced into a triple quadrupole mass spectrometer (TSQ Ultra, Thermo Scientific) using a chip-based nano-ESI source (Advion NanoMate) operating in infusion mode. PC lipids were measured using precursor ion scanning of *m/z* 184. Quantification of lipid molecular species was performed using the Lipid Mass Spectrum Analysis (LIMSA) software version 1.0 peak model fit algorithm. Three to four samples per genotype were analyzed for comparison.

80.2.4 Electroretinography

Electroretinography (ERG) was performed under scotopic conditions as previously described [6]. Briefly, anesthetized 7-month-old mice were subjected to 10 msec flashes of light of increasing intensities (0.004 to 400 cd.s/m^{-2}). The maximum amplitudes of rod-only a-waves (Rmp^3) were determined by analyzing the ERG responses as previously described [7]. Data were processed with MatLab software (MathWorks, Inc). The maximum rod b-wave (V_{max}) amplitude was determined as the least squares fit of log intensity vs. amplitude response analysis according to the previously described Naka-Rushton equation [8]. Photopic ERG was determined as response amplitudes (b-wave) to a single flash (2,000 cd.s/m^2) and to continuous pulses of different frequencies of light (5–30 Hz).

80.2.5 Statistical Analysis

Two-way ANOVA followed by Bonferroni's multiple comparison test was used to analyze ERG responses. All other data were analyzed by Students 2-tailed t-test. Analyses were performed using GraphPad (GraphPad Prism, Inc), with statistical significance set at $p < 0.05$.

80.3 Results

80.3.1 Cre Recombinase Eliminated ELOVL4 Expression from Rods in RcKO Retina

Immunolabeling of retinal wholemounts confirmed cell-specific expression of Cre in the RcKO retina (Fig. 80.1a) and demonstrated specific deletion of ELOVL4 from rods

expressing Cre (Fig. 80.1b). Cre labeling showed a mosaic distribution in the rods of the RcKO mice that corresponded to the mosaic pattern of ELOVL4 deletion (Fig. 80.1b). As a rough estimate of the extent of Cre-mediated *elovl4* deletion in the RcKO retina, the proportion of the ONL occupied by labeling for ELOVL4 indicated that ELOVL4 was eliminated from approximately 40–60 % of the ONL, consistent with the 36 % reduction of VLC-PUFA observed by tandem mass spectroscopy (see fig. 80.1).

80.3.2 Retinal Phosphatidylcholine VLC-PUFA Analysis

Tandem mass spectrometry analysis showed a smaller amount of PC VLC-PUFA (54:11 to 56:12) in 9-month-old RcKO retinas compared to the WT control retinas (Table 3.1). The only VLC-PUFA-containing species in the RcKO retina that was significantly reduced compared to WT retina was 56:11 (22:6/34:5) (Table 3.1). However, the total amount of PC VLC-PUFA in the RcKO retina was 36 % lower than WT littermates ($p < 0.001$). PC VLC-PUFA precursors (44:12 to 46:12) were more abundant in the RcKO mouse retina compared to WT retina, but 44:11 (22:6/22:5) was the only species that differed significantly (Table 3.1).

80.3.3 ERG Analysis

Scotopic ERG was performed on WT and RcKO mice to determine whether the reduction in VLC-PUFA levels affected the rod photoresponse. There were no differences in a- and b-wave amplitudes between WT and RcKO mice at any of the light intensities used (Fig 80.2a). Similarly, there were no significant differences between the WT and RcKO Rmp_3 (421 and 359 μV; $p > 0.05$) values, although the Vmax in RcKO (828 μV) mice was significantly lower than in WT (919 μV; $p = 0.049$; Fig 80.2b). Cone ERG responses to a single flash (2,000 cd.s/m^2) in light-adapted WT and RcKO mice (161 and 127 μV, respectively; Fig. 80.2c), and photopic flicker ERG responses did not differ significantly between the WT and RcKO mice (Fig. 80.2c).

80.4 Discussion

We used mice with rod-specific deletion of *Elovl4* to investigate the role of VLC-PUFA in rod photoreceptors. Heterogeneous ELOVL4 deletion was consistent with the known mosaic expression of Cre in the rods of the transgenic mouse line used to create the RcKO strain used here [3]. ELOVL4 deletion in the RcKO mice resulted in a 36 % reduction in retinal PC VLC-PUFA (Table 80.1), whereas VLC-PUFA precursors (44:11 to 46:12) were more abundant in the RcKO mouse retina compared to WT (Table 80.1). The “back up” of lipid species agrees with results of Harke-wicsz et al. who showed higher amounts of precursors 44:12, 44:11, and 46:11 in their rod-specific *Elovl4* cKO compared to WT mouse retina [9].

We found no differences in area occupied by ONL in 9- and 15-month-old WT and RcKO mice (data not shown). These analyses indicate that the reduction of VLC-PUFA in the RcKO mice did not cause rod cell death. These results differ from those of Harkewicsz et al., who reported that 10- and 15-month-old RcKO mice had 8 and 7 rows of photoreceptor nuclei, respectively, compared to 9 rows of nuclei in their 15-month-old WT mice [9]. In that study, the numbers of rows of photoreceptor nuclei in the ONL were counted at two

points, 500 μm superior and inferior to the ONH on frozen sections of 16 μm thickness. In the current study, we measured the area occupied by the entire ONL across the vertical meridian of the entire retina in paraffin sections of 5 μm thickness. The reason for these differences is not obvious as both studies used the same rod cre-expressing mice. However, the measurement approach utilized in the current study samples a much larger area of the ONL with higher anatomical resolution and minimizes effects of orientation in relatively thick frozen sections that can make assignment of individual photoreceptor nuclei to a specific row difficult.

Rod ERG responses were comparable for WT and RcKO mice at all light intensities tested (Fig. 80.2a). The rod-only response (Rmp3) was lower in the RcKO than WT mice, but was not statistically significant ($p = 0.0503$; Fig. 80.2b). However, the Vmax was significantly lower in the RcKO mice compared to WT ($p = 0.049$; Fig. 80.2b). Harkewicsz et al. reported that the scotopic ERG response from RcKO mice was lower than the WT response to a light intensity of 0.0084 cd.s/m^2 [9], an intensity between two used in our study (0.004 and 0.4 cd.s/m^2), neither of which elicited statistically different responses from our WT and RcKO mice. This difference potentially might reflect the age of mice used. The mice we used were 7 months of age, but no age was given for the mice used by Harkewicsz et al., [9]. Perhaps with increasing age, our RcKO mice might also show a decline in ERG responses. The mosaic deletion of *Elovl4* by Cre also might affect the ERG results as heterogeneous photoreceptor dysfunction can bias ERG responses [10]. Cone function assessed by photopic ERG responses did not differ between RcKO and WT mice (Fig. 80.2c). These results agree with those reported by Harkewicsz et al., who showed that mice with rod-specific *Elovl4* deletion had a photopic 10 Hz flicker ERG response comparable to WT mice [9]. These results suggest that the level of VLC-PUFA reduction in the RcKO retina did not alter rod or cone function by 7 months.

A 36 % reduction in VLC-PUFA was not sufficient to cause photoreceptor cell death or rod or cone dysfunction. Our analyses of VLC-PUFA levels in retinas of *Elovl4* KO and *Elovl4* knock-in (KI) heterozygous mice showed ∼ 50 % reduction compared to WT (Mandal et al., unpublished results). The KO mice have no structural phenotype at 16 to 22 months-of-age [11] and the KI mice had minimal ERG changes and normal retinal morphology at 8 and 9 months-of-age [12, 13]. Importantly, these KO and KI mice differ from those used in the current study because the reduction in VLC-PUFA levels occurs in each rod cell, since each expresses only one WT copy of *Elovl4*. In the RcKO mice, rod cells express either two or zero copies of Elovl4, which would result in each cell having either “normal” or very low levels of VLC-PUFA. Recent studies in which we deleted *Elovl4* from over 90 % of rods showed a structural and functional phenotype at 4 months-of-age (Marchette, unpublished results). Thus, in the present study, we would expect to find some phenotype in the rods of the animals in which *Elovl4* was deleted, unless there was transfer of VLC-PUFA between cells. One potential mechanism for this transfer would be recycling of VLC-PUFA from the shed tips of rod outer segments through the retinal pigment epithelium (RPE) to cells lacking *Elovl4*. This recycling phenomenon is well-known for DHA [1, 6] and retinoids involved in the visual cycle [14].

In summary, partial reduction of VLC-PUFA in rod photoreceptors is not sufficient to cause a structural or functional retinal phenotype. Even though VLC-PUFA synthesis was completely eliminated in some individual rod cells, these cells did not appear to be deleteriously affected, most likely because of sharing of these fatty acids through their efficient recycling from the RPE.

Acknowledgments

This work was supported by NIH Grants EY00871, EY04149, EY12190, EY21725, EY22071 and RR17703; Foundation Fighting Blindness, Inc., and Research to Prevent Blindness, Inc.

References

1. Zhang K, et al. A 5-bp deletion in ELOVL4 is associated with two related forms of autosomal dominant macular dystrophy. Nat Genet. 2001; 27:89–93. [PubMed: 11138005]
2. Agbaga MP, Brush RS, Mandal MNA, Henry K, Elliott MH, Anderson RE. Role of Stargardt-3 macular dystrophy protein (ELOVL4) in the biosynthesis of very long chain fatty acids. Proc Nat Acad Sci. 2008; 105(35):12843–12848. [PubMed: 18728184]
3. Le YZ, Zheng L, Zheng W, Ash JD, Agbaga MP, Zhu M, et al. Mouse opsin promoter-directed Cre recombinase expression in transgenic mice. Mol Vis. 2006; 12:389–398. [PubMed: 16636658]
4. Mojumder DK, Frishman LJ, Otteson DC, Sherry DM. Voltage-gated sodium channel alpha-subunits Na(v)1.1, Na(v)1.2, and Na(v)1.6 in the distal mammalian retina. Mol Vis. 2007; 13:2163–2182. [PubMed: 18079688]
5. Busik JV, Reid GE, Lydic TA. Global analysis of retina lipids by complementary precursor ion and neutral loss mode tandem mass spectrometry. Methods Mol Biol. 2009; 579:33–70. [PubMed: 19763470]
6. Li F, Marchette LD, Brush RS, Elliott MH, Le YZ, Henry KA, et al. DHA does not protect ELOVL4 transgenic mice from retinal degeneration. Mol Vis. 2009; 15:1185–1193. [PubMed: 19536303]
7. Hood DC, Birch DG. Rod phototransduction in retinitis pigmentosa: estimation and interpretation of parameters derived from the rod a-wave. IOVS. 1994; 35(7):2948–2961.
8. Naka KI, Rushton WA. S-potentials from luminosity units in the retina of fish (Cyprinidae). J Physiol. 1966; 185(3):587–599. [PubMed: 5918060]
9. Harkewicz R, Du H, Tong Z, Alkuraya H, Bedell M, Sun W, et al. Essential role of ELOVL4 protein in very long chain fatty acid synthesis and retinal function. J Biol Chem. 2012; 287(14): 11469–11480. [PubMed: 22199362]
10. Hood DC, Shady S, Birch DG. Understanding changes in the b-wave of the ERG caused by heterogeneous receptor damage. IOVS. 1994; 35(5):2477–2488.
11. Raz-Prag D, Ayyagari R, Fariss RN, Mandal MNA, Vasireddy V, Majchrzak S, et al. Haploinsufficiency is not the key mechanism of pathogenesis in a heterozygous Elovl4 knockout mouse model of STGD3 disease. IOVS. 2006; 47(8):3603–3611.
12. Li W, Chen Y, Cameron DJ, Wang C, Karan G, Yang Z, et al. Elovl4 haploinsufficiency does not induce early onset retinal degeneration in mice. Vis Res. 2007; 47(5):714–722. [PubMed: 17254625]
13. McMahon A, Butovich IA, Mata NL, Klein M, Ritter R 3rd, Richardson J, et al. Retinal pathology and skin barrier defect in mice carrying a Stargardt disease-3 mutation in elongase of very long chain fatty acids-4. Mol Vis. 2007; 13:258–272. [PubMed: 17356513]
14. Chen H, Ray J, Scarpino V, Acland GM, Aguirre GD, Anderson RE. Synthesis and release of Docosahexaenoic acid by the RPE cells of prcd-affected dogs. Invest Ophthalmol Vis Sci. 1999; 40(10):2418–2422. [PubMed: 10476811]

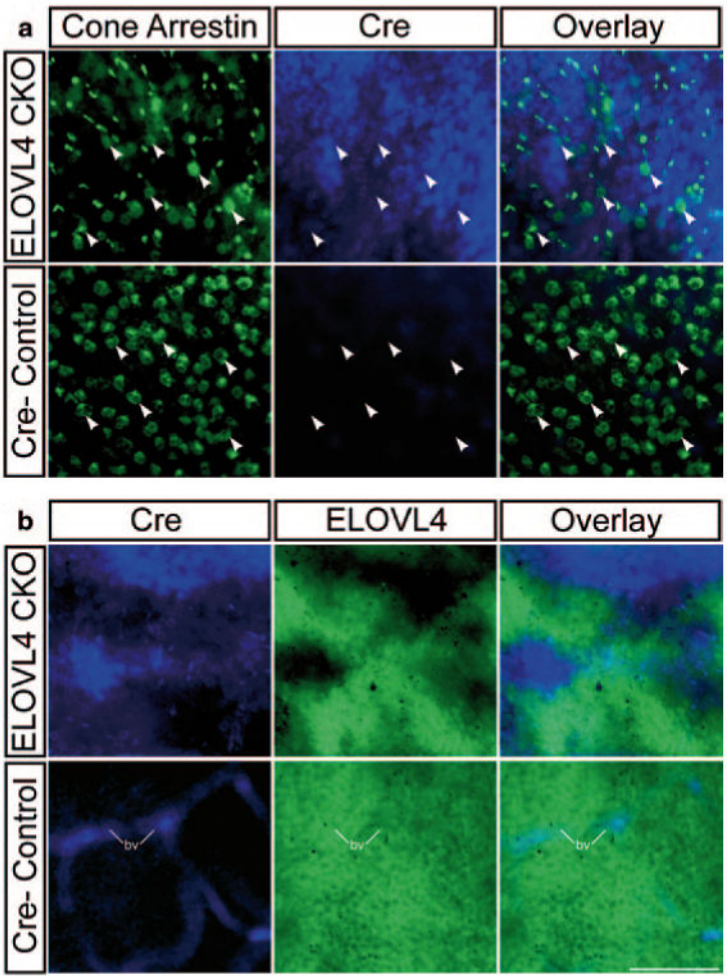

Fig. 80.1.

Rod-specific deletion of ELOVL4. **a** Immunolabeling for Cone *Arrestin* (*green*) and *Cre* (*Cre; blue*) identified the persistence of cones (*arrowheads*) and confirmed rod-specific *Cre* expression in the RcKO retina (*ELOVL4 CKO*) that was absent from the Cre negative control retina (*Cre-Control*). **b** Cre (*blue*) expression in the RcKO retina showed mosaic distribution that corresponded to the deletion of ELOVL4 (*green*). In contrast, Cre labeling was absent in the *Cre-Control* retina, while *ELOVL4* was present in all photoreceptors. Labeling of blood vessels (*bv*) in the Cre channel was non-specific. Scale bar = 50 μm

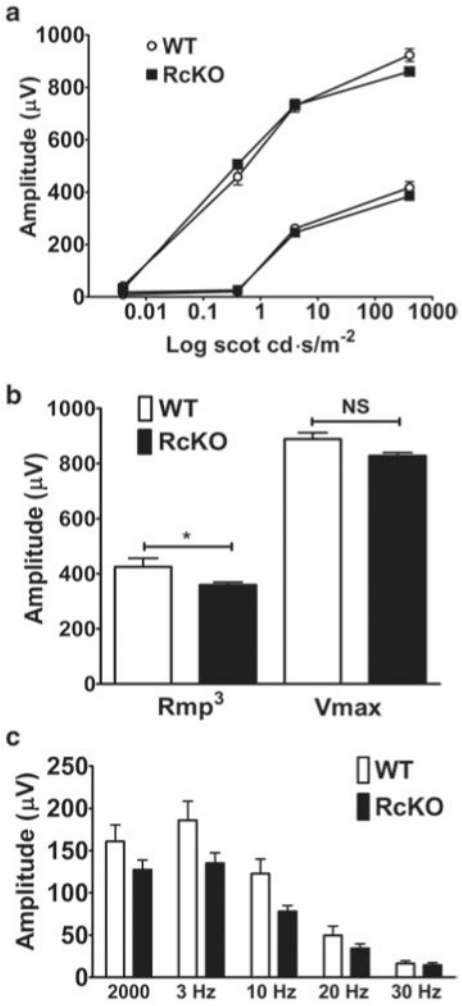

Fig. 80.2.

Electroretinography responses. **a** Scotopic ERG a- (*lower* lines) and b- (*upper* lines) waves were comparable between wild-type (*WT*) and rod-specific *Elovl4* knockout (*RcKO*) mice. **b** Maximum a- (Rmp^3) and b- (V_{max}) wave responses were lower in the *RcKO* compared to *WT* but not to a level of statistical significance. **c** *WT* and *RcKO* had comparable cone responses (b-waves) to phot-opic single flash (2,000 cd.s/m^2) and flicker (5–30 Hz) ERGs. $p > 0.05$ for all phot-opic ERG responses. $n = 4–5$ different *WT* and *RcKO* mice respectively for all ERG. Data is mean response amplitudes (μV) ± SEM

Table 80.1

Retinal phosphatidylcholine analysis

Name	WT	RcKO
44:11* (22:6/22:5)	0.09 ± 0.02	0.14 ± 0.02
44:12 (22:6/22:6)	3.92 ± 1.79	6.15 ± 0.88
46:11 (22:6/24:5)	0.06 ± 0.07	0.10 ± 0.09
46:12 (22:6/24:6)	0.30 ± 0.09	0.31 ± 0.04
54:11 (22:6/32:5)	0.17 ± 0.06	0.13 ± 0.04
54:12 (22:6/32:6)	0.75 ± 0.35	0.58 ± 0.22
56:11** (22:6/34:5)	0.17 ± 0.02	0.00 ± 0.00
56:12 (22:6/34:6)	0.41 ± 0.10	0.26 ± 0.08

RcKO rod conditional *Elovl4* knockout, *WT* wild type

* $p < 0.05$;

** $p < 0.001$